TECHNICAL ARTICLE

Uninstrumented Measurement Method for Granular Porous Media Blast Mitigation Assessment

A.-N. Rotariu[1], C. Dima[1], E. Trană[1], C. Enache[1], F. Timplaru[2], and L.-C. Matache[3]

1 Faculty of Mechatronics and Integrated Armament Systems, Military Technical Academy, Bucharest, Romania
2 In Flight Research & Test Center, Gherceşti, Romania
3 Scientific Research Center for CBRN Defense and Ecology, Bucharest, Romania

Keywords
Blast Wave, Pressure, Impulse, Plate Deformation, Perlite

Correspondence
A.-N. Rotariu,
Faculty of Mechatronics and Integrated Armament Systems,
Military Technical Academy,
39-49 George Cosbuc Ave.,
District 5,
050141 Bucharest
Romania
Email: arotariu99@yahoo.com

Received: May 23, 2014;
accepted: February 16, 2015

doi:10.1007/s40799-016-0099-4

Abstract

The current paper is concerned with testing the efficiency of a uninstrumented method in assessing granular porous media capacity to mitigate blast impulse. A thin plate constant deformation test was carried out based on the findings obtained throughout blast–structure interaction phenomena. The proposed test requires only post-test measured data and no test instrumentation is needed. The test protocol under scrutiny consists of a short series of 200 g TNT charge detonations at 1000 mm distance from the tested structures. All test results have shown impulse mitigation. The findings obtained in the test under scrutiny tally those in the pendulum test. The final section of the current article is concerned with the improvement and shortcomings of the test developed.

Introduction

Unwanted blast events involving high explosives such as terrorist attacks with improvised explosive devices (IED) or unexploded ordnances (UXO) and demining accidents represent a security threat to our present day society. During high explosive detonation phenomena, gases are generated at a pressure of up to 300 kbar and a temperature of about 3000–4000°C. These hot gases expand, and most of the released energy forms a layer of compressed air (blast wave) in front of this gas volume.[1] When the explosive is enveloped in a metallic enclosure, the energy is transferred to the enveloping material, resulting in fragmentation and high-velocity shrapnel. Such events may also initiate secondary fires.

Given the potential threat mentioned above, the need arose for protecting buildings, cars, and other goods and for mitigating the devastating effects of the blast waves. Over the past decades, considerable research has been carried out on ballistic effects on protective structures,[2] interactions of blast waves with various materials, and fire retardant materials.[3] With respect to blast attenuation, research has been focused on identifying effective mechanisms for blast energy dissipation and containment of explosive overpressure using blast-mitigating materials. Solutions proposed for attenuation and reflection of shock waves and high-energy flows included use of permeable solids, porous materials, and solid geometric reflectors.[4] Various media that have been used in research include energy-absorbing or energy-dissipating foams,[5] liquids encapsulated in elastic shells, textiles, cellular materials, resin-bonded aggregates, honeycomb structures,[6] perforated plates,[7] and granular media.

An important observation regarding material performance can be made from various experimental studies[5,8]: only very careful and judicious use of protective material will ensure blast mitigation. Otherwise, if mitigation material is too thin, soft, and has a large porosity, the overpressure and impulse transferred to the structure can be amplified.[9]

As mentioned above, the property of a material to mitigate blast wave effects is estimated by

measuring the overpressure P_s in front of the shock wave and the impulse I transferred to a structure, both with and without the protective layer under investigation. Pressure measurements are usually done with piezoelectric transducers in face-on or side-on positions, while the impulse is measured using the pendulum principle in horizontal or vertical configurations.[5,10,11] When thin, deformable plates are subjected to blast loads, accelerometers can be used to instrument the test specimens.[8] The more recent digital image correlation approach employs high-speed cameras with the view to measuring instantaneous displacement and velocity of deformable plates.[12–14]

The thin plate behavior under blast loading scenarios has been addressed by numerous researchers. An important finding demonstrated experimentally through regression analysis[15,16] was the linear dependence between loading impulse and permanent deformation at plate center, both in circular and rectangular plates. Analytical models[17,18] and recent experimental work on scaling[10,11,19–22] reinforce the findings of previous studies.

Porous and granular media have long been recognized as a cost-effective solution for conducting blast mitigation research.[8,23–25] Perlite, an amorphous volcanic glass was used in the current work, in which the advantage of this mineral's property to undergo significant structural modification under thermal loading was put to use. The modified structure combines high porosity and low density with a granular state. The correspondent mechanical behavior, specific to crushable plasto-elastic material,[23] ensures a blast wave mitigation effect when perlite is exposed to blast loading. Perlite behavior under blast loading has been characterized by previous researchers whose results are available in published literature.[26] An important observation related to perlite behavior is the fact that expanded perlite aggregate is highly dependent on raw material. Perlite obtained from two different sources with the same densities and gradations can produce two widely different crushing strengths.[23]

Previous experimental work on blast effects on perlite as a function of layer thickness was conducted by the authors and results were published elsewhere.[27] In addition to a standard test configuration using a single layer of porous medium, tests were conducted on a more complex configuration, which consisted of two layers of porous media separated by air. The results confirmed the perlite's capability for blast wave mitigation, which was in line with results published by other research groups.[26] A reduction of blast wave pressure was also observed during tests, ranging between 0.78 and 0.95 of baseline readings. Measurements of blast wave pressure attenuation showed good consistency with layer thickness. Specific impulse reduction did not show similar consistency. Moreover, data acquisition from several tests was affected by unexpected out-of-scale signal evolution and, therefore, no impulse value was calculated. The 95% overpressure attenuation recorded on the dual perlite layer separated by air was considered as a promising result as it slightly exceeded the performance of a single layer.

The above-mentioned challenges related to pressure transducer use for measurements of pressure and impulse reduction justified the search for a new impulse mitigation evaluation method, which is investigated throughout the current research work. The article proposes using thin deformable plates as eyewitnesses in blast loads, given the linear dependence that has been demonstrated between maximum permanent deflection of the center of a thin plate and transferred blast wave impulse.

Blast Wave—Obstacle Interaction

As shown in Fig. 1, typical blast pressure profile at a certain distance from the point of detonation is characterized by sharp increases to a peak value of overpressure, P_s, above ambient pressure, P_0. The pressure then decreases to a value less than P_0, generating partial vacuum before eventually returning to ambient conditions.[1]

Throughout the pressure–time profile, two main phases can be observed[1]: the first one above ambient pressure (positive phase) and the second one below ambient pressure (negative phase). Positive phase duration t_d has been correlated with the standoff distance R and charge weight W.[28] The relationship between t_d and R is of a linear type in logarithmic terms, and may be approximated conservatively by Eq. (1).

$$\log_{10}\left(\frac{t_d}{\sqrt[3]{W}}\right) \approx -2.75 + 0.27\log_{10}\left(\frac{R}{\sqrt[3]{W}}\right) \quad (1)$$

The blast wave propagation causes outward air movement following the shock front at a lower velocity. The movement of air particles creates wind pressure that depends on the peak overpressure of the blast wave. Air velocity is associated with dynamic pressure $q(t)$. The maximum value q[29] is given by

$$q = \frac{5P_s^2}{2\,(7P_0 + P_s)} \quad (2)$$

The shock wave is reflected by objects or structures encountered on its way.[1] The reflection factor

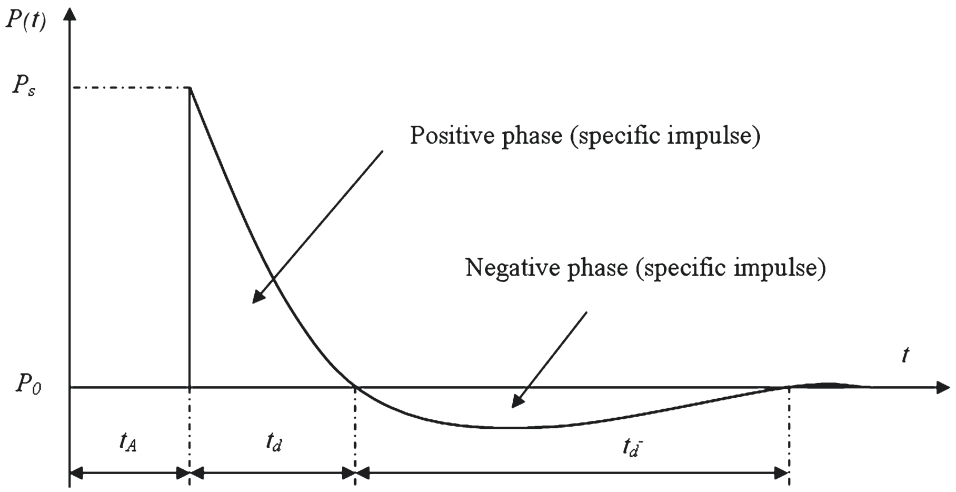

Figure 1 Blast wave pressure.

depends on the shock wave intensity and on the angle of incidence.[28,30] If the blast wave encounters an obstacle perpendicular to the direction of propagation, the reflection will increase the overpressure to a maximum reflected pressure[29] P_r:

$$P_r = 2P_s \frac{7P_0 + 4P_s}{7P_0 + P_s} \tag{3}$$

Shock wave–structure interactions are not characterized exclusively by reflected pressure.[30] Due to the shock wave reflection on the front face of the obstacle, a rarefaction wave is developed to reduce the excess pressure. This pressure relief will start at the edge of the obstacle and spread inward toward its center. The new pressure value is stagnation overpressure, which is defined as[30]

$$P_{stag} = P_s + q \tag{4}$$

The time measured from the beginning of blast loading until the stagnation pressure reaches the center of the obstacle is given approximately by[30]

$$t' = \frac{3d}{2U} \tag{5}$$

where d is the smallest obstacle size and U blast front (shock) velocity. This phenomenon triggers a modification in pressure acting on the obstacle. Blast wave interaction can be further influenced by variations in shape and nature of the obstacles encountered: walls, buildings, cars, etc. For example, pressures estimated through numerical simulations at the center of a cylindrical obstacle are shown in Fig. 2 for a range of obstacle diameters.[31] The shock wave was produced by a TNT charge of 0.5 kg at 1 m distance. Although the pressure profile is identical

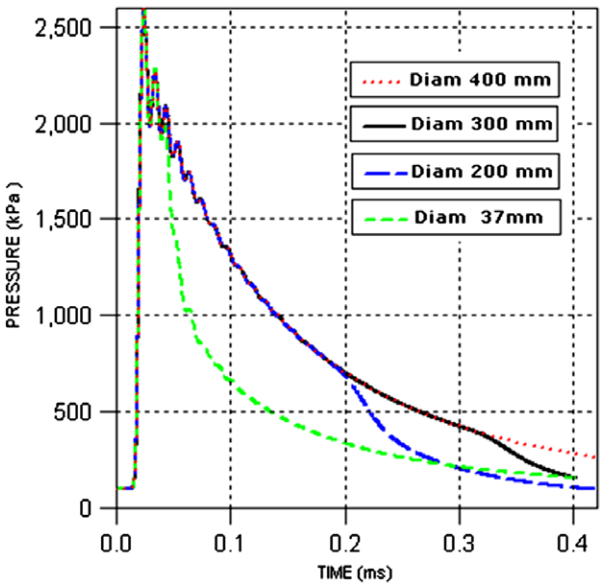

Figure 2 Pressure decay recorded for 37, 200, 300, and 400 mm diameter.

in all cases during the initial phase, the pressure decreases that follow are influenced by the obstacle diameter. The earliest and the most abrupt decrease is recorded for a 37 mm diameter mount.

The next section focuses on two main cases: (A) interactions with square, immovable thin deformable plates and (B) movable rigid plates in a pendulum rig.

Immovable thin deformable plates: case (A)

The first case deals with square thin plates. The experimental work on permanent inelastic deformation of

plates subject to blast loading consists of a large number of tests.[16] An empiric linear relationship between relative permanent deflection of plate center and a dimensionless damage number φ_q is given through mathematical regression in[16]:

$$\delta/h = 0.48\varphi_q + 0.277 \tag{6}$$

where δ is the permanent deflection of plate center, h stands for plate thickness, and φ_q is given by the following relationship

$$\varphi_q = \frac{I}{2h^2\sqrt{bl\rho\sigma_0}} \tag{7}$$

The value of the dimensionless damage number is given by blast loading conditions through impulse I and by plate dimensions through plate thickness h, lateral dimensions b and l, plate material density ρ, and material static yield stress σ_0. A schematic view of this test, also used in our test plan, is represented in Fig. 3(a).

In Eq. (6) applied to relative deformations higher than 10, the 0.277 contribution becomes less than 3%, which is an acceptable error margin in blast-related measurements. In such cases, the 0.277 contribution may be neglected, allowing Eq. (6) to be rewritten as

$$\delta/h = 0.48\varphi_q \tag{8}$$

Equation (8) allows comparison between large deformations on two identical thin plates:

$$\frac{\delta_1}{\delta_2} = \frac{\varphi_{q1}}{\varphi_{q2}} = \frac{I_1}{I_2} \tag{9}$$

Equation (9) shows that for large deformations, the ratios between the center deflections and the plate-transferred impulses may be seen as equals.

Movable rigid plates: case (B)

The second case investigated movable rigid plates in a pendulum rig. The hypothesis and the mathematical relationships for the experimental determination of impulse are detailed in Hanssen et al.[5] The hypothesis of pendulum initial movement conditions, which is purely translation movement or purely rotation movement, leads to different relationships and consequently different values of impulse[5]:

$$I_l = \sqrt{2M_p^2 gd\,(1-\cos\theta_{max})} \tag{10}$$

$$I_r = \frac{1}{s}\sqrt{2C_W M_p gd\,(1-\cos\theta_{max})} \tag{11}$$

Except for the maximum deflection angle θ_{max} and the gravitational acceleration g, all other terms in Eqs. (10) and (11) are related to pendulum design and test setup: M_p is the pendulum mass; C_w is moment of inertia about the rotational axis of the pendulum; d is the distance between the center of mass and the rotational axis; s is the distance between charge location and the rotational axis, as in Fig. 3(b). In both cases, a relative comparison between two tests with the same pendulum data is related only to the maximum angle of pendulum deflection:

$$\frac{I_{l1}}{I_{l2}} = \frac{I_{r1}}{I_{r2}} = \sqrt{\frac{1-\cos\theta_{1\,max}}{1-\cos\theta_{2\,max}}} \tag{12}$$

Moreover, as long as rotational angles are small enough, less than 0.25π *rad*, relative comparison can be made, with sufficient precision, by simply dividing the maximal angles

$$\frac{I_{l1}}{I_{l2}} = \frac{I_{r1}}{I_{r2}} \approx \frac{\theta_{1\,max}}{\theta_{2\,max}} \tag{13}$$

This approximation is justified by the nature of the $\sqrt{1-\cos\theta}$ curve within the $[0, 0.25\pi]$ $\times$ *rad* interval, which is characterized by linearity. Figure 4 presents graphically the linearity argument, through comparison with the linear curve $0.69^*\theta$. In quantitative terms, the difference between $\sqrt{1-\cos\theta}$ and $0.69^*\theta$ functions never exceeds 2% within the $[0, 0.25\pi]$ $\times$ *rad* interval.

Test Protocol

In the test program, an expanded perlite grade was used as a protective layer, similar to previously reported work.[27] The material was characterized experimentally with respect to granule shape and size distribution, as well as its mechanical behavior. The average bulk density was determined to be 63.2 kg/m^3. Samples of perlite were sifted using an automatic sieve, which allowed to establish the particle size distribution. Figure 5 presents the mass distribution. A small percentage of perlite has a size more than 1 mm. A microscopic analysis revealed irregular grain shapes and a fine porous structure. The test protocol was completed by tri-axial compression tests (compressibility test). Typical exhibit behavior is illustrated in Fig. 6 and is representative for crushable plasto-elastic materials, having no distinct yield point and some degree of compressibility.

The test plan is mainly based on the conclusion from the previous section regarding direct proportionality between the impulse and thin plate deformation. A series of experimental tests using unprotected plates and perlite-covered plates illustrated the capability of perlite for blast impulse mitigation, evaluated using

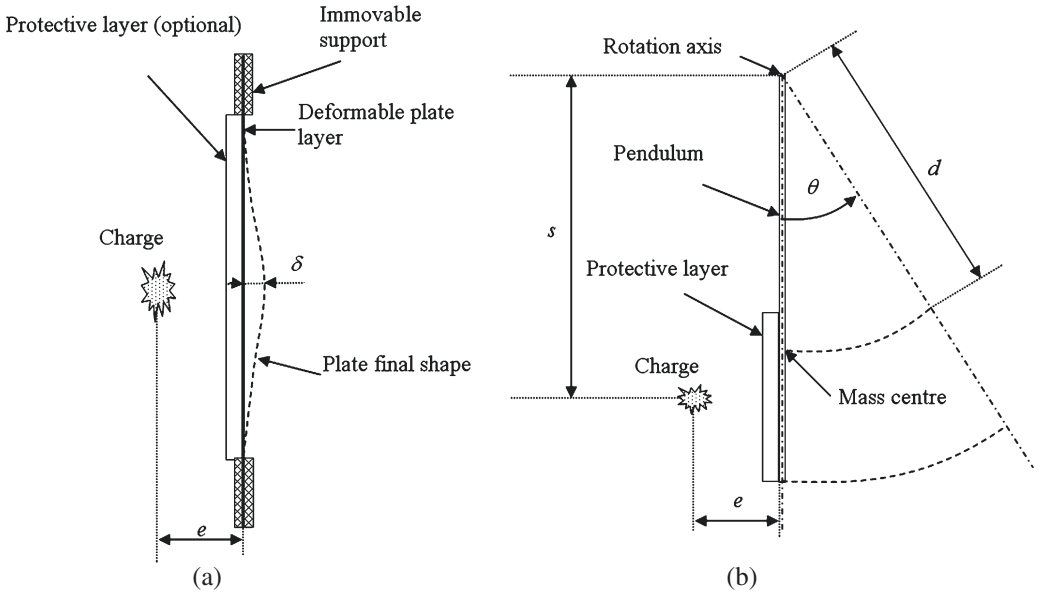

Figure 3 Schematic view of test configurations: deformable plate test (a) and blast-loaded pendulum (b).

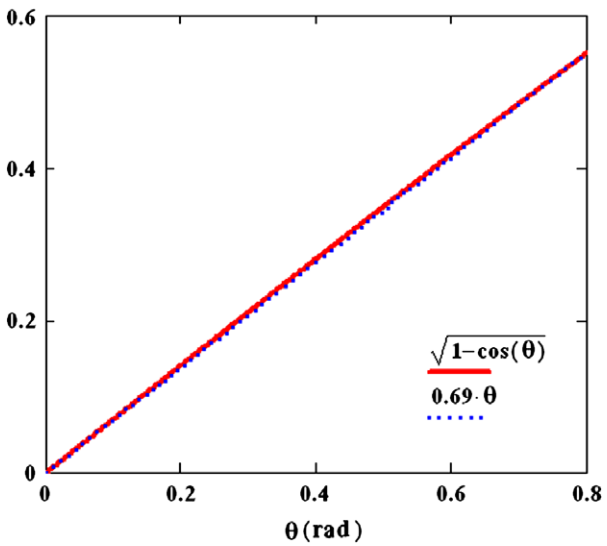

Figure 4 Linearity evaluation of $\sqrt{1-\cos\theta}$ curve.

Eq. (9). In order to validate the experimental test results, experimental tests using the pendulum principle were also included in the test plan.

For both types of experimental tests, the same rig was employed, including a $20 \times 1000 \times 1200$ mm steel plate. A 400×400 mm square hole was cut out in the center. Two mounting systems were designed in order to clamp thin plates in front of the hole and attach the pendulum behind. The structure was firmly anchored to the ground. Lateral considerable dimensions of structure were chosen in order to prevent the apparition of stagnation pressure on the samples during the positive blast wave phase. The first configuration with deformable plates uses structural steel (S235 grade) plates of 1 mm thickness. The plates were clamped between a 12 mm thick steel cover and the 20 mm thick steel support plate and were fixed with screws placed around the plates. No screw passes through deformable plates.

The pendulum was attached to the back side of the structure. The total length of the pendulum was 700 mm and the plate of the pendulum had $400 \times 400 \times 12$ mm dimensions. The pendulum plate was positioned right behind the square hole of the support plate. The pendulum weighed 17.5 kg and the distance between its rotational axis and the mass center was 480 mm. The perlite layers had different thicknesses and were enclosed in wooden boxes with side plastic covers. The perlite boxes were attached in front of the structure hole for both types of tests. Details of the experimental test setup are presented in Fig. 7.

A TNT charge of 200 g made up of two cylindrical 100 g charges, placed side-by-side, was used in all experimental tests. The charges were situated at 1000 mm distance from the structure for all experimental tests.

An M102 blunt piezoelectric pressure transducer was used for blast wave measurement in air at 1000 mm distance from the detonation point. An axial accelerometer was mounted at the center of the structural steel plates to measure the acceleration. A 39 g mass was added (the transducer and the

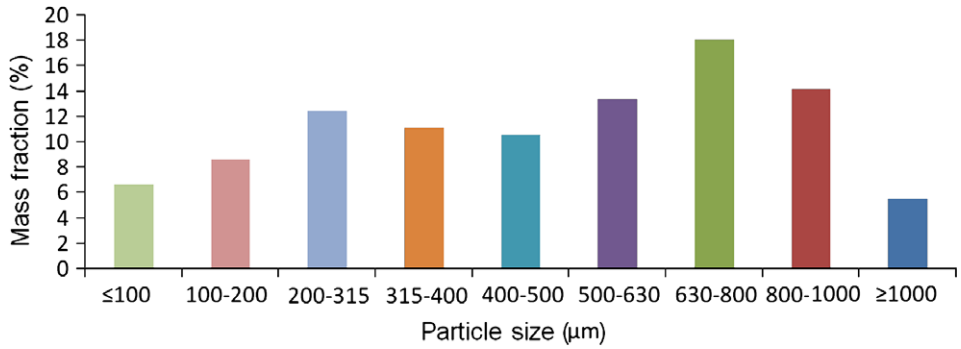

Figure 5 Perlite grain size distribution.

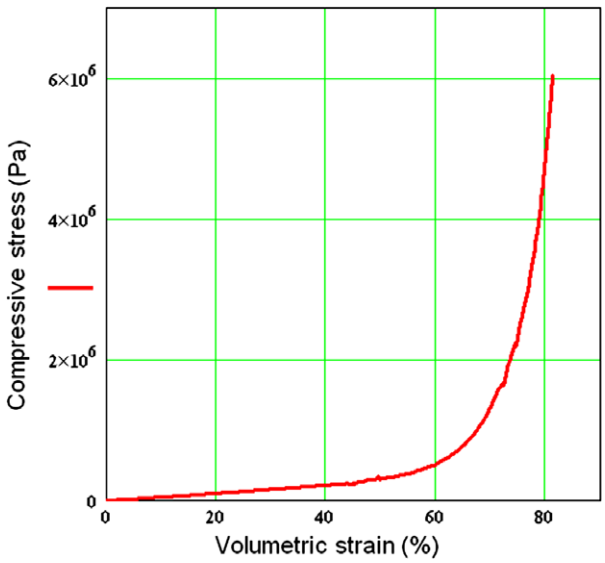

Figure 6 Compression-strain diagram for expanded perlite of 0.0632 g/cm^3 density.

screw support). Both accelerometer and pressure transducer signals were acquired with a PicoScope® 6 – PC Oscilloscope (Pico Technology Limited, St Neots, UK). In all tests, the signals were acquired at 10 MHz sample rates. The pressure transducers were mounted in a face-on position. In the so-called face-on measurements, the sensitive surface of a pressure transducer is positioned parallel to the blast wave front, so that the pressure behind the reflected wave P_r is actually measured and the related value for the incident blast is deduced using the normal shock relationship. Blast pressure was recorded for all experimental tests and plate acceleration was also recorded, though only for the tests on deformable plates.

All experimental tests were recorded with FASTCAM (Photron Limited, Tokyo, Japan), a high-speed camera, at 20,000 frames/s. The rotation angles of the pendulum were obtained from the images recorded. The precision of this method is considered sufficient as long as these values are used to validate mitigation capability, calculated using the method proposed in the present study. Such method is quick although not highly precise. In each case, the frame that was used for calculation, which corresponds to pendulum stop, was chosen by a frame by frame analysis. The position of the pendulum was determined through calculations with data obtained by manual choosing of pixels. The pixels were selected along the pendulum edge.

Considering the extremely low velocities, the camera time of exposure does not affect the pendulum position recorded in the frame used for calculations. Manual choice of pixels may produce some errors, but there is no reason to presume that this will somehow affect the results of tests for large angle values.

The test protocol is presented in Table 1, which also indicates the type of test and perlite layer thicknesses.

Experimental Results and Discussions

The maximum blast wave overpressure recorded by the eyewitness transducer was approximately 0.9 MPa in all experimental tests.

As expected, the acceleration measured at the center of plate was affected by the presence of the perlite layer. The acceleration profiles measured on deformable plates can be seen in Fig. 8. For the bare plate test, three regions can be identified. The first one, of around 1 m length, is characterized by a plateau with oscillations between 20,000 and 35,000 m/s^2. A second region is a rise at a higher value than the plateau value, over 40,000 m/s^2, followed by a sharp decrease down to less than negative 60,000 m/s^2, which marks the third region. If the first region is clearly related to pressure action on plate, the

Figure 7 Details of test setup.

Table 1 Test protocol and results

Test no.	1	2	3	4	5	6	7
TNT charge	200 g	200 g	200 g	200 g	200 g	200 g	200 g
Perlite box thickness	–	15 cm	5 + 5 cm	10 cm	10 cm	—	15 cm
Test type	Plate	Plate	Plate	Plate	Plate	Pendulum	Pendulum
Permanent deflection/maximum rotation angle	23.1 mm	10.5 mm	18.8 mm	16.7 mm	14.2 mm	25.7°	12.6°
Mitigation	–	54.5%	18.6%	27.7%	38.5%	—	50.4% 51%

following two are more likely to be the effects of plate deceleration, which starts from clamped edges and spreads inward toward the plate center. The plate deceleration phenomenon was observed using high-speed video. For the remaining tests on perlite-protected plates, the recorded accelerations were lower than those measured on bare plate test.

Permanent deflections at plate centers were measured and the results are presented in Table 1. The maximum permanent deflections were measured with a caliper after the plates were cut. Undeformed region plates clamped on the test rig were used as ''0 displacement'' reference. Using Eq. (9), impulse mitigation was calculated individually for each experimental test, using the value from test no. 1 as baseline, in the denominator. A maximum mitigation factor of 54.5% was observed in test no. 2 for a perlite box of 15 cm thickness. There is some difference between the test results on 10 cm thick perlite boxes: 27.7% mitigation estimated (per Eq. (9)) for one sample and 38.5% for the other. The experimental test on 5 cm thick perlite boxes separated by a 5 cm gap shows a poor mitigation performance of only 18.6%. Figure 9 shows side views of all five plates.

The discrepancy between the result of test no. 5 and the results presented in a previously reported research[27] is not necessarily unlikely as long as the obtained impulse mitigation has usually lower values than overpressure mitigation. The test no. 3 acceleration history, after a low start, shows an intermediary increase that may represent the effect of perlite first layer that is accelerated by blast wave and pressure on second layer. The secondary growth indicates the increase of the momentum transferred to the plate, and consequently, the central permanent deflection is larger. Further investigations such as numerical simulations are needed to determine the reason for this discrepancy.

Images captured for the two experimental tests with pendulum were used for estimation of a maximal angle deflection, as shown in Fig. 10. The maximum angular deflection in the test with a bare pendulum was 25.7°, while a 12.6° value was recorded in the test using a 15 cm thick layer of perlite.

The impulse mitigation estimated using Eq. (12) equals 50.4%, very close to 51%, which was estimated using Eq. (13).

The granular state and porosity of the perlite imply fundamental difficulties in the understanding of its intrinsic dynamic properties due to the strong nonlinearity and complex contact-force distributions between grains. Plastic deformation, pore collapse,

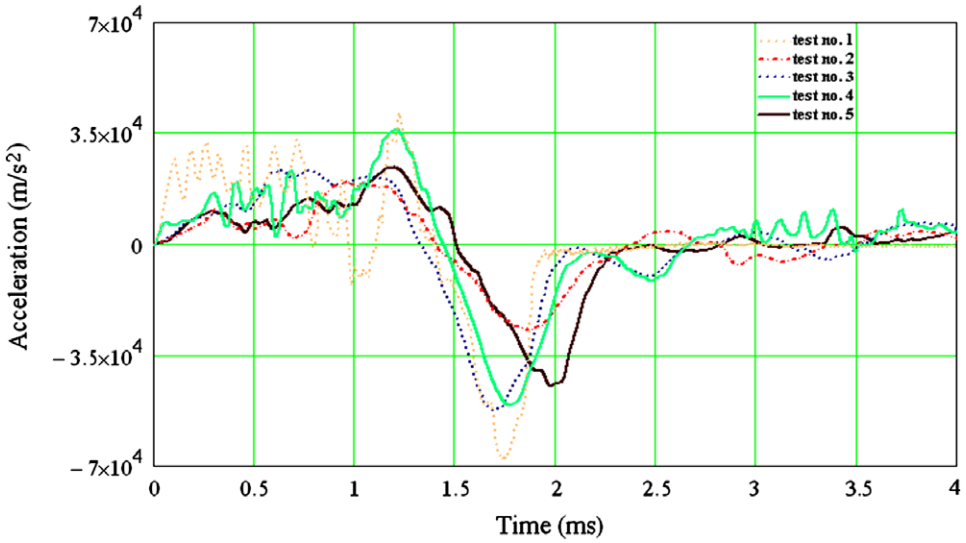

Figure 8 Plate center acceleration for tests no. 1–5.

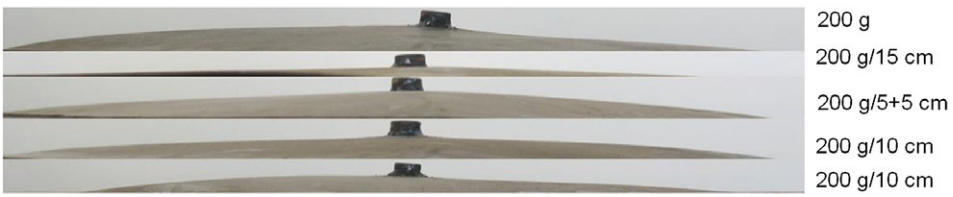

Figure 9 Deflection of plates for tests no. 1–5.

and grain comminution are different mechanisms of energy dissipation, which can take place in perlite. All the above-mentioned characteristics and mechanisms are reflected in a macroscale characteristic, compression-volumetric strain curve, as shown in Fig. 6. The characteristic curve gives an overall view on the perlite potential to absorb shock energy. The specific energy absorbed by perlite is the area under this curve.

The experimental work conducted using the test configuration described above confirmed the blast-mitigating property of perlite, if present in a layer of sufficient thickness. Generalizing this conclusion for test scenarios other than 200 g TNT explosive charges at 1000 mm distance is not recommended because it has been shown previously that inadequate use of protective material can actually increase the blast impulse transferred to the structure.[9]

A secondary outcome of this study is related to the proposed test configuration, which produced very similar impulse mitigation measurements as a standard pendulum setup. In particular, estimates of the blast-mitigating capability of a 15 cm layer of perlite were 54.5% using thin deformable plates and 51% using a pendulum setup, which are extremely close for this type of experiments.

The most appealing aspect of this method is not its precision, but rather the inexpensive nature of the setup: no test instruments such as pressure transducers, movement transducers, accelerometers, or high-speed cameras are necessary to estimate impulse mitigation. The proposed setup allows a quick estimate of the performance of a protective layer, without requiring expensive and time-consuming preparation steps, which are prerequisite of other competing measurement techniques.

The 39 g added weight due to accelerometer attachment to the plate center may have some impact on the acceleration profile; however, the effect on the permanent deflection at the center is not clear. A comparison between the proposed test results and the pendulum test results suggests that even if there exists such an effect, it must be proportional to blast loading conditions and final deflection; therefore, blast mitigation estimates using the two methods are likely similar. Future work using numerical simulations is planned to clarify this issue.

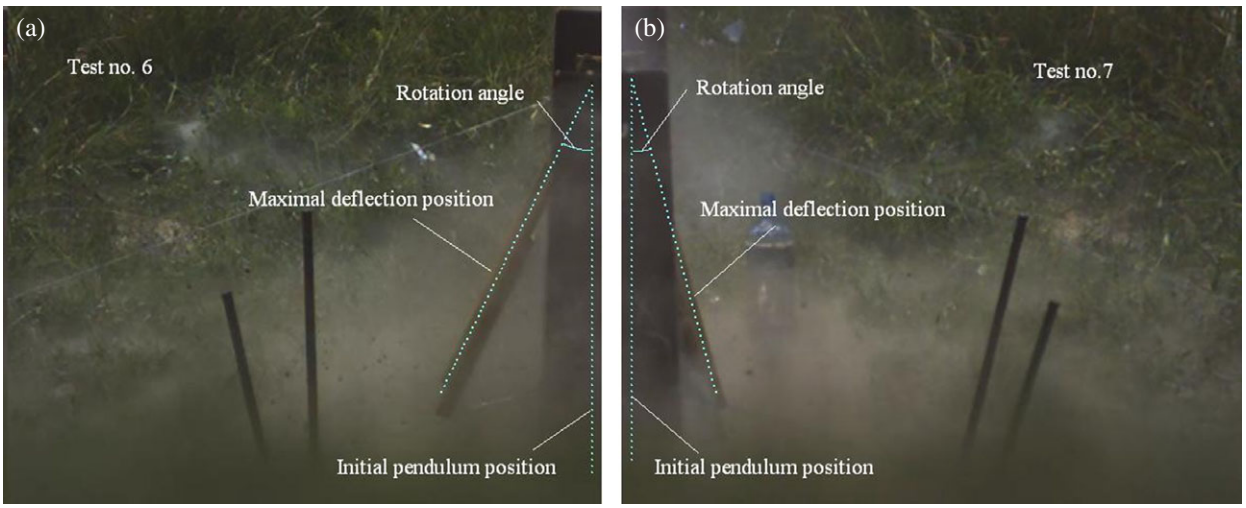

Figure 10 Comparison of maximal deflection angles for tests 6(a) and 7(b).

The test on a two-layer perlite sample, separated by a gap, revealed an impulse mitigation of only 18.6%, which is a less promising result than overpressure mitigation found in a previously reported study.[27]

The tests based on 10 cm thick perlite layers show inconsistent results for virtually identical test conditions. Errors associated with the test setup may have led to this discrepancy. The difference between test 4 and 5 measurements may be attributable to a possible misalignment of the charge, or a small change in the location of the detonation point in the charge, relative to the obstacle. Another factor may be inherent variations in material properties and blast loading conditions or even blasting cap performance that are known to have significant impact on test results.

The current study measured the impact of a blast load on a single plate, and future tests are being considered to use a mirror setup, exposing to the same blast two different test samples: a bare plate and a second plate covered by a protective layer. Equation (9) may then be applied to data recorded during the same test, which will eliminate the effects of inherent variability in blast loading conditions from one test to another.

The limited number of test samples may represent the main drawback of the current experimental research. Additional tests are being planned to further investigate the mitigating properties of the perlite and its potential limitations. Such studies will improve the understanding of perlite behavior under blast loading. Leveraging the advantages of this protective material (low cost, low labor content manufacturing, and low density) will produce clear benefits for defense and commercial security applications.

Conclusion

The experimental findings of this study have shown that relative blast impulse mitigation obtained in the presence of granular layer may be estimated with acceptable precision by the permanent central deflection of an eyewitness square plate.

The analytical and empirical mathematical relationships, related to blast impulse effect on pendulum structure and deformable plates, developed and proposed by others researchers, were used for reasoning on the proposed method.

The tests protocol consists of a series of 200 g TNT detonations at standoff distance of 1000 mm. Perlite layers of various thicknesses were used as protective layer and 400×400 mm steel plates of 1 mm thickness as eyewitness plates. Interpretation of tests results (central permanent deflection), based on the new proposed assessment method, indicates mitigation of blast impulse. The protective layer thickness influences the impulse mitigation value. When using two air-gap thin perlite layers, the result indicates poor performance.

For validation, a pendulum test was carried out for 15 cm perlite layer thickness. The impulse mitigation of 51% assessed by pendulum test has a similar value to that obtained with the newly proposed method, 54.5%.

References

1. Ngo, T., Mendis, P., Gupta, A., and Ramsay, J., ''Blast Loading and Blast Effects on Structures, An Overview,'' *Electronic Journal of Structural Engineering, Special Issue: Loading on Structures*: 76–91 (2007).

2. Dulgheriu, I., Avădanei, M., Badea, S., and Safta, I., ''Experimental Research on Establishing the Level of Bullets Protection for a Ballistic Protection Structure,'' *Industria Textilă* **63**(4):198–203 (2012).
3. Rotariu, T., Zecheru, T., Rusen, E., Goga, D., and Cincu, C., ''Kinetic Study of A New Flame-Retardant Polymer Composition,'' *Materiale Plastice* **48**(1):83–87 (2011).
4. Seeraj, S., and Skews, B.W., ''Dual-Element Directional Shock Wave Attenuators,'' *Experimental Thermal and Fluid Science* **33**(3):503–516 (2009).
5. Hanssen, A.G., Enstock, L., and Langseth, M., ''Close-Range Blast Loading of Aluminium Foam Panels,'' *International Journal of Impact Engineering* **27**(9):593–618 (2002).
6. Wadley, H.N.G., ''Multifunctional Periodic Cellular Metals,'' *Royal Society of London Transactions Series A* **364**(1838):31–68 (2006).
7. Langdon, G.S., Nurick, G.N., Balden, V.H., and Timmi, R.B., ''Perforated Plates as Passive Mitigation Systems,'' *Defence Science Journal* **58**(2):238–247 (2008).
8. Guéders, C., Van Roey, J., Gallant, J., and Coghe, F., ''Simulation of Shock Wave Mitigation in Granular Materials by Pressure and Impulse Characterization,'' *Proceedings of the 8th European LS-DYNA Users Conference*, Dynamore GmbH, Strasbourg, France; May 23-24, 2011, Session 15, Paper 3.
9. Nesterenko, V.F., ''Shock (Blast) Mitigation by ''Soft'' Condensed Matter,'' *Proceedings of Matter Research Society Symposium: Granular Materials-Based Technologies*, Materials Research Society, Boston, MA; December 2–5, 2002, Vol. 759, MM 4.3.1–4.3.12.
10. Fourney, W.L., Leiste, U., Bonenberger, R., and Goodings, D., ''Mechanism of Loading on Plates due to Detonation,'' *International Journal for Blasting and Fragmentation* **9**(4):205–217 (2005).
11. Fourney, W.L., Leiste, U., Bonenberger, R., and Goodings, D., ''Explosive Impulse on Plates,'' *International Journal for Blasting and Fragmentation* **9**(1):1–17 (2006).
12. Zhao, X., Tiwari, V., Sutton, M.A., et al., ''Scaling of the Deformation Histories for Clamped Circular Plates Subjected to Buried Charges,'' *International Journal of Impact Engineering* **54**:31–50 (2013).
13. Zhao, X., Hurley, R., Sutton, M.A., et al., ''Small Scaled Models Subjected to Buried Blast Loading Part I: Floorboard Accelerations and Related Passenger Injury Metrics With Protective Hulls,'' *Experimental Mechanics* **54**(4):539–555 (2014).
14. Arora, H., Hooper, P.A., and Dear, J.P., ''Blast Loading of Sandwich Structures and Composite Tubes, Dynamic Failure of Composite and Sandwich Structures,'' Abrate, S., *et al.*, (eds), *Solid Mechanics and Its Applications*, Springer, Netherlands, Volume 192, pp. 47–92 (2013).
15. Nurick, G.N., and Martin, J.B., ''Deformation of Thin Plates Subjected to Impulsive Loading a Review, Part I: Theoretical Considerations,'' *International Journal of Impact Engineering* **8**(2):159–169 (1989).
16. Nurick, G.N., and Martin, J.B., ''Deformation of Thin Plates Subjected to Impulsive Loading a Review, Part II: Experimental Studies,'' *International Journal of Impact Engineering* **8**(2):171–186 (1989).
17. Lee, Y.W., and Wierzbicki, T., ''Fracture Prediction of Thin Plates under Localized Impulsive Loading. Part I: Dishing,'' *International Journal of Impact Engineering* **31**(10):1253–1276 (2005).
18. Lee, Y.W., and Wierzbicki, T., ''Fracture Prediction of Thin Plates under Localized Impulsive Loading, Part II: Discing and Petalling,'' *International Journal of Impact Engineering* **31**(10):1277–1308 (2005).
19. Jacob, N., Yuen, S.C.K., Nurick, G.N., Bonorchis, D., Desai, S.A., and Tait, D., ''Scaling Aspects of Quadrangular Plates Subjected to Localized Blast Loads Experiments and Predictions,'' *International Journal of Impact Engineering* **30**(8–9):1179–1208 (2004).
20. Neuberger, A., Peles, S., and Rittel, D., ''Scaling the Response of Circular Plates Subjected to Large and Close-Range Spherical Explosions, Part I: Air-Blast Loading,'' *International Journal of Impact Engineering* **34**(5):859–873 (2007).
21. Neuberger, A., Peles, S., and Rittel, D., ''Scaling the Response of Circular Plates Subjected to Large and Close-Range Spherical Explosions, Part II: Buried Charges, Air-blast Loading,'' *International Journal of Impact Engineering* **34**(5):874–882 (2007).
22. Jacob, N., Nurick, G.N., and Langdon, G.S., ''The Effect of Stand-Off Distance on the Failure of Fully Clamped Circular Mild Steel Plate Subjected to Blast Loads,'' *Engineering Structures* **29**(10):2723–2736 (2007).
23. Hoff, G.F., *Shock Absorbing Materials*, U.S. Army Engineer Waterways Experiment Station, Vicksburg, MS, Report No. 6-673 (1967).
24. Walley S.M., and Proud, W.G., ''A Comparison of the Quasistatic and Dynamic Compressibilities of Wet and Dry Vermiculite,'' *Proceedings of 9th International Conference on the Mechanical and Physical Behaviour of Materials under Dynamic Loading*, DYMAT, EDP Sciences, Brussels, Belgium; September 7–11, 2009, pp. 331–336.
25. Grujicic, M., Pandurangan, B., Bell, W.C., and Bagheri, S., ''Shock-Wave Attenuation and Energy-Dissipation Potential of Granular Materials,'' *Journal of Materials Engineering and Performance* **21**(2):167–179 (2012).

26. Nesterenko, V.F., *Dynamics of Heterogeneous Materials*, Springer-Verlag, New York, NY, pp. 276–277 (2001).
27. Rotariu, A., Trana, E., Timplaru, F., Matache, L., Badea, S., and Chereches, T., ''On Attenuation Properties of Blast Wave through Perlite,'' *Proceedings of the 14th International Conference ModTech International Conference—New face of TMCR*, Nedelcu D., (eds), Technical University Gheorghe Asachi of Iasi, ModTech Publishing House, Iasi, Romania; May 20–22, 2010, pp. 499–502, 2010.
28. Lam, N., Mendis, P., and Ngo, T., ''Response Spectrum Solutions for Blast Loading,'' *Electronic Journal of Structural Engineering* **4**:28–44 (2004).
29. Mohanty B., *Physics of Explosion Hazards, Forensic Investigation of Explosions*, 2nd, A. Beveridge, Taylor & Francis Ltd, Bridgeport, NJ, 28–40, 2011
30. Smiyh, P.D., and Hetherington, J.G., *Blast and Ballistic Loading of Structures*, Butterworth and Heinemann Ltd., Oxford, UK, pp. 44–56 (1994).
31. Matache, L., Rotariu, A., Paschia, L., Safta, I., ''A Dimensional Analysis of Transducers Mounts Used in Measurements of Impulsive Loads of Structures,'' *Proceedings of the 17th International Conference the Knowledge-Based Organization*, ''Nicolae Balcescu'' Land Forces Academy, ''Nicolae Balcescu'' Land Forces Academy Publishing House, Sibiu, Romania; November 24–26, 2011, pp. 110–114.